



## High rate reactive magnetron sputter deposition of titanium oxide

T. Kubart, D. Depla, D. M. Martin, T. Nyberg, and S. Berg

Citation: [Applied Physics Letters](#) **92**, 221501 (2008); doi: 10.1063/1.2938054

View online: <http://dx.doi.org/10.1063/1.2938054>

View Table of Contents: <http://scitation.aip.org/content/aip/journal/apl/92/22?ver=pdfcov>

Published by the [AIP Publishing](#)

---



## Re-register for Table of Content Alerts

Create a profile.



Sign up today!



## High rate reactive magnetron sputter deposition of titanium oxide

T. Kubart,<sup>1,a)</sup> D. Depla,<sup>2</sup> D. M. Martin,<sup>1</sup> T. Nyberg,<sup>1</sup> and S. Berg<sup>1</sup>

<sup>1</sup>The Ångström Laboratory, Uppsala University, P.O. Box 534, SE-751 21 Uppsala, Sweden

<sup>2</sup>Ghent University, Department of Solid State Sciences, Krijgslaan 281(S1) 9000 Gent, Belgium

(Received 3 March 2008; accepted 23 April 2008; published online 2 June 2008)

A systematic experimental study of reactive sputtering from substoichiometric targets of  $\text{TiO}_x$  with  $x$  ranging from 0 to 1.75 is reported. Experimental results are compared with results from modeling. The developed model describes the observed behavior and explains the origins of the unexpectedly high deposition rate. The behavior is shown to originate from the presence of titanium suboxides at the target surface caused by preferential sputtering of the oxide. The model can be used for optimization of the target composition with respect to the deposition rate and film composition in a stable hysteresis-free reactive sputtering process. © 2008 American Institute of Physics. [DOI: 10.1063/1.2938054]

Reactive magnetron sputtering is a widely used deposition technique for oxide coatings. It has many applications due to its simplicity, versatility, and possibility to be scaled up for large-area coatings. However, the inherent instabilities indicated by the hysteresis effect limits the achievable compositions or decreases the deposition rate substantially. There is a continuous effort by many researchers trying to overcome this problem without the use of a complex feedback control of the reactive gas partial pressure.<sup>1-3</sup> Recently, results have been published regarding  $\text{TiO}_2$  films deposited from  $\text{TiO}_{1.8}$  sputtering targets.<sup>4</sup> The main reason for using such a target was its conductivity which enabled dc sputtering. A substantially higher deposition rate, compared to that from a metal target operated in compound mode, was reported, and the results also indicated elimination of hysteresis. The sputtering process using such a target has been studied by Hoshi and Takahashi<sup>5</sup> analyzing both film properties and composition of the sputtered particles. The results have confirmed previous findings but no clear and generally valid explanation of the effect has, however, been given. In this letter, we report on a study of reactive sputtering from  $\text{TiO}_x$  targets of various composition together with the modeling of the process.

The depositions were carried out by reactive dc magnetron sputtering from a 2 in. target in the constant current ( $I=160$  mA) mode onto Si substrates without additional heating. An effective pumping speed of 16 l/s and argon flow of 4 sccm (SCCM denotes cubic centimeter per minute at STP) was used. The mass deposition rate was measured by a quartz crystal microbalance. Targets were sintered from a mixture of  $\text{TiO}_2$  and Ti powders: the composition is shown in Table I. In the text below, we refer to the original composition of the powder mixture. The oxygen loss is caused by heating during the sintering process.<sup>6</sup>

Typical hysteresis curves for metal targets are shown in Fig. 1 (solid line). The abrupt transition from high rate metal mode to compound mode, with substantially lower mass deposition rate, occurs at a flow of 0.6 sccm of  $\text{O}_2$  [Fig. 1(b)]. The transition is accompanied by an equally abrupt change in the discharge voltage, as shown in Fig. 1(a), due to a change of target surface composition.<sup>7</sup> The magnitude of

the hysteresis depends on the material (sputtering yields and reactivity) and the configuration of the sputtering system (target size, pumping speed, etc.).

From experimental observations, it can be seen that with an increasing amount of oxide in the target, the hysteresis is reduced and eventually disappears. It is also clearly seen that the nearly stoichiometric target, dotted line in Fig. 1, has a high mass deposition rate in pure Ar. The rate seen here is about 50% of the metal rate. Even when taking into account the difference in discharge voltage, this shows that the nearly stoichiometric target has a quite high sputter yield. This technologically interesting fact should be addressed when modeling this process. However, existing models<sup>8</sup> of the sputtering process fail to reproduce this observed behavior (not shown here).

$\text{TiO}$  and  $\text{Ti}_2\text{O}_3$  may be created at the surface by reduction of  $\text{TiO}_2$  under ion bombardment as revealed by photoelectron spectroscopy.<sup>9</sup> In order to account for the  $\text{TiO}_2$  reduction, the existence of another phase at the target was implemented into the standard model. Therefore, the pres-

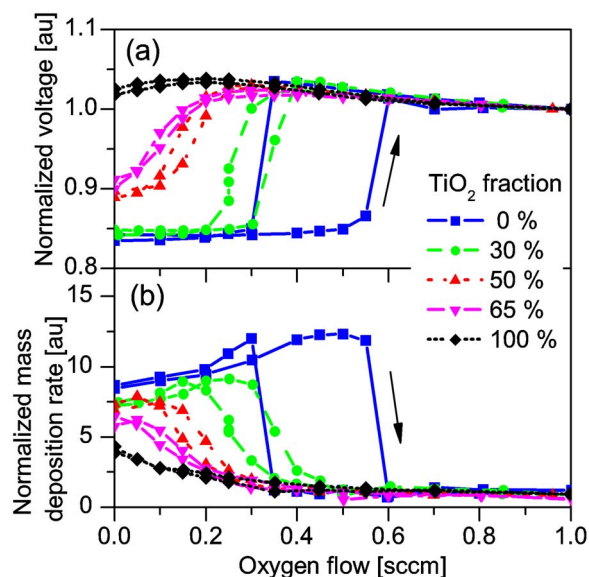


FIG. 1. (Color online) (a) Target voltage and (b) mass deposition rate for five different compositions of the sputtering target. Values are normalized to the value at 1 sccm of  $\text{O}_2$  (in fully poisoned mode).

<sup>a)</sup>Electronic mail: Tomas.Kubart@angstrom.uu.se.

ence of metallic Ti, stoichiometric TiO<sub>2</sub>, and a lower oxide is assumed. There are several possible stoichiometries of the lower oxides, namely Ti<sub>2</sub>O<sub>3</sub> and TiO. In our model, only one phase, Ti<sub>2</sub>O<sub>3</sub>, is assumed. This is in agreement with the reported absence of metallic Ti at the bombarded oxide surface and substantially lower conversion rate of Ti<sub>2</sub>O<sub>3</sub> to TiO than TiO<sub>2</sub> into Ti<sub>2</sub>O<sub>3</sub>.<sup>9</sup> Therefore, congruent sputtering is assumed for Ti and O from Ti<sub>2</sub>O<sub>3</sub>.

As the values of the sputtering yields are crucial input parameters, for the simplified model presented in this work, a binary collision approximation (BCA) has been used for sputtering yield calculations. BCA is routinely used to describe ion/solid interaction for sputtering yield calculations. In this work, the program Transport of Ions in Matter (TRIM) from The Stopping and Range of Ions in Matter (SRIM) 2006 package was used.<sup>10</sup> TRIM is a static program, where the target composition is fixed and not influenced by ion bombardment. Here, it is used to describe the sputtering of individual phases present at the target surface. The actual evolution of target composition is accounted for in the reactive model. The most influential parameter of TRIM calculations is the surface binding energy  $U_s$ , describing the surface potential. This value is, however, not usually known for compound targets and an approximation based on the heat of atomization is commonly used.<sup>11</sup> Such an approach cannot be used for oxides as the calculated values of sputtering yields for compounds are substantially larger than the experimental values. From the ratio of mass deposition rate in metal and compound mode, as shown in Fig. 1(b), the Ti sputtering yield from the compound surface can be estimated to be at least eight times lower than the yield from the metallic surface. Kelly<sup>12</sup> used point-defect theory and predicted a substantially higher value of  $U_s$  for metal than for oxygen in ionic oxides. In the case of Ti, the calculations are more complicated due to the change in valence during the transition between different Ti oxides. Experimental studies of Ti atoms sputtered from O covered surface have indicated the value of 16 eV for the surface binding energy of Ti in TiO<sub>2</sub>.<sup>13</sup> The surface binding energy of O given by Samsonov is 7 eV.<sup>14</sup>

The reactive model is based on the assumptions reviewed by Berg and Nyberg.<sup>8</sup> Only equations for the balance of the target composition are shown here; the others are equivalent to the equations shown elsewhere.<sup>2</sup> In steady state, the creation of each target phase is balanced for by its removal through sputtering. The Ti and Ti<sub>2</sub>O<sub>3</sub> may react with O<sub>2</sub> and form Ti<sub>2</sub>O<sub>3</sub> and TiO<sub>2</sub>, respectively, with a probability given by the flux of neutral reactive molecules,  $F$ , and the corresponding sticking coefficient  $\alpha$ .<sup>8</sup> TiO<sub>2</sub> may be reduced by ion impact due to the preferential sputtering of oxygen. Sputtering of all phases is described by corresponding sputtering yields, assuming atomic sputtering i.e., each element sputters with a given partial sputtering yield from a corresponding compound. Material sputtered from the target is replaced by the exposed bulk material, which consists of metal and a fraction of TiO<sub>2</sub>,  $\theta_b^{\text{TiO}_2}$ , according to the actual

composition shown in Table I. The target balance equations are

$$\begin{aligned} &4/3 \times \alpha F (1 - \theta_t^{\text{Ti}_2\text{O}_3} - \theta_t^{\text{TiO}_2}) + 2 \times I/q_e Y_{\text{O}}^{\text{TiO}_2} \theta_t^{\text{TiO}_2} \\ &= 4\alpha^{\text{Ti}_2\text{O}_3} F \theta_t^{\text{Ti}_2\text{O}_3} + I/q_e Y^{\text{Ti}_2\text{O}_3} \theta_t^{\text{Ti}_2\text{O}_3} \end{aligned} \quad (1)$$

and

$$\begin{aligned} &4\alpha F \theta_t^{\text{Ti}_2\text{O}_3} + I/q_e [Y^{\text{Ti}_2\text{O}_3} \theta_t^{\text{Ti}_2\text{O}_3} + Y_{\text{Ti}}^{\text{Ti}} (1 - \theta_t^{\text{Ti}_2\text{O}_3} \\ &- \theta_t^{\text{TiO}_2})] \theta_b^{\text{TiO}_2} = 2I/q_e Y_{\text{O}}^{\text{TiO}_2} \theta_t^{\text{TiO}_2} \\ &+ I/q_e Y_{\text{Ti}}^{\text{TiO}_2} \theta_t^{\text{TiO}_2} (1 - \theta_b^{\text{TiO}_2}), \end{aligned} \quad (2)$$

where the Eq. (1) represents the balance of  $\theta_t^{\text{Ti}_2\text{O}_3}$ , the part of surface covered by Ti<sub>2</sub>O<sub>3</sub>, and Eq. (2) describes the balance of surface covered by TiO<sub>2</sub>,  $\theta_t^{\text{TiO}_2}$ . An explanation of all symbols together with values used in the presented work is shown at the end of the letter. The system of equations can be used to obtain the dependence of process parameters on the oxygen pressure. Hence, the results show the complete hysteresis curve including unstable points inside the transition area.

TRIM calculations give the sputtering yield of Ti from TiO<sub>2</sub> as 0.037 and 0.12 for O. The deviations from the values used in the analytical model might be due to several factors. TRIM calculations depend critically on the input surface binding energy, which could be influenced by the actual surface composition different from pure stoichiometric TiO<sub>2</sub>.<sup>15</sup> The results from TRIM therefore give an indication rather than absolute values of the sputtering yield. There are also a number of simplifications assumed in the model. The sputtering yield of Ti<sub>2</sub>O<sub>3</sub> was used as a free parameter as there are no experimental measurements available.

Results of the proposed model are shown in Fig. 2. The simulated results agree very well with experimental mass deposition rates for all target compositions. The high deposition rate is connected with the presence of Ti<sub>2</sub>O<sub>3</sub> at the target surface,  $\theta_t^{\text{Ti}_2\text{O}_3}$  in Fig. 2(b). Even for a stoichiometric TiO<sub>2</sub> target, a substantial fraction of Ti<sub>2</sub>O<sub>3</sub> is created at the surface due to the preferential sputtering of oxygen in pure Ar (not shown). However, as the TiO<sub>2</sub> is insulating, no direct experimental comparison in dc mode of operation is possible. The resulting mass deposition rate for an oxide target in pure argon is comparable to that of a metal target due to a relatively higher surface fraction of Ti<sub>2</sub>O<sub>3</sub>, which is in agreement with experimental findings.

If the process is hysteresis-free, in our case, for more than 50 wt % of TiO<sub>2</sub> in the initial powder mixture, a stable operating point exists for all oxygen flows, as shown in Fig. 2(c). A substantial fraction of Ti<sub>2</sub>O<sub>3</sub> may be maintained at the target even for a process without partial pressure control while depositing stoichiometric TiO<sub>2</sub> at the substrate at a very high rate. This is very important for industrial applications due to the possibility to increase the deposition rate of the oxide in comparison to a metal target operated in compound mode. The necessary condition for such process is a hysteresis-free operation, which can be achieved using tar-

TABLE I. The powder composition for production of targets and the actual target composition as measured by Rutherford backscattering spectroscopy.

TiO <sub>2</sub> (wt. %)	0	30	50	65	100
x in TiO <sub>2</sub>	0	0.4	0.75	1.0	1.75

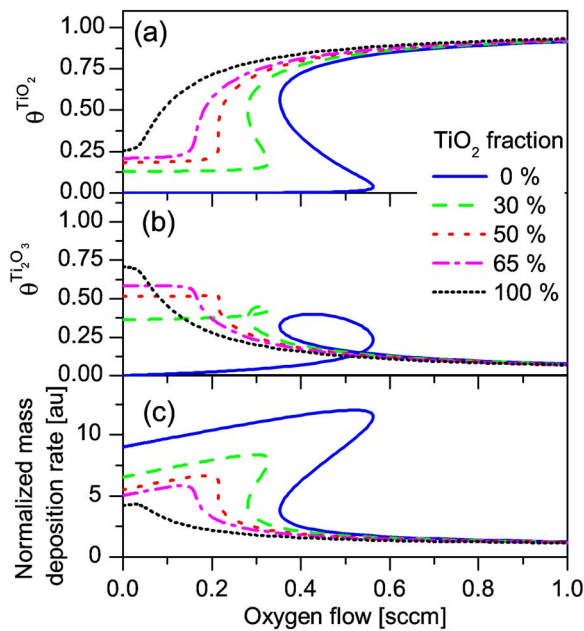


FIG. 2. (Color online) Simulated target surface composition, coverage with (a)  $\text{TiO}_2$ , and (b)  $\text{Ti}_2\text{O}_3$ , and the (c) normalized mass deposition rate for different target stoichiometries.

gets with a certain fraction of oxide. The required composition depends on other parameters in a sputtering setup, but the composition may be predicted using the developed model.

Even a further increase in the deposition rate may be achieved by using a target with an optimum composition. This is illustrated in Fig. 3, showing a simulated composition of the coatings together with mass deposition rate (lines with symbols). For the 65% target, an additional increase in deposition rate compared to the most oxygen rich (100% target case) is predicted. The mass deposition rate for stoichiometric  $\text{TiO}_2$  films is about 35% higher than the corresponding rate from 100% target. The developed model can be used to find the optimum target composition for a particular deposition system giving the highest possible deposition rate of compound films in a hysteresis-free process. Similar behavior is expected for other metals which form suboxides.

The following parameters have been used for the simulations: Discharge current  $I=160$  mA, effective target area  $A_t=8$  cm<sup>2</sup>, effective substrate area  $A_s=400$  cm<sup>2</sup>, sputtering

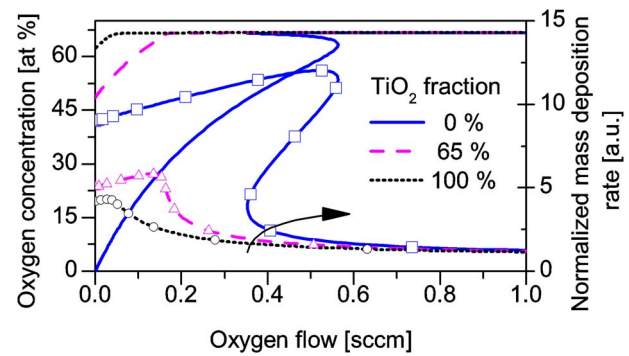


FIG. 3. (Color online) Simulated composition of sputtered films and corresponding mass deposition rate (lines with symbols) for three different target compositions.

yield of O from  $\text{TiO}_2$ ,  $Y_{\text{O}}^{\text{TiO}_2}=0.14$ , Ti from  $\text{TiO}_2$ ,  $Y_{\text{Ti}}^{\text{TiO}_2}=0.018$ , Ti from  $\text{Ti}_2\text{O}_3$ ,  $Y_{\text{Ti}}^{\text{Ti}_2\text{O}_3}=0.10$ , and sticking coefficient of  $\text{O}_2$ ,  $\alpha=1$ .  $q_e$  denotes the electron charge.

This work was supported by the Swedish Foundation for Strategic Research (SSF) Strategic Research Center in Materials Science for Nanoscale Surface Engineering (MS2E).

- <sup>1</sup>T. Nyberg, S. Berg, U. Helmersson, and K. Hartig, *Appl. Phys. Lett.* **86**, 164106 (2005).
- <sup>2</sup>D. Severin, O. Kappertz, T. Kubart, T. Nyberg, S. Berg, A. Pflug, M. Siemers, and M. Wuttig, *Appl. Phys. Lett.* **88**, 161504 (2006).
- <sup>3</sup>W. D. Sproul, D. J. Christie, and D. C. Carter, *Thin Solid Films* **491**, 1 (2005).
- <sup>4</sup>H. Ohsaki, Y. Tachibana, A. Mitsui, T. Kamiyama, and Y. Hayashi, *Thin Solid Films* **392**, 169 (2001).
- <sup>5</sup>Y. Hoshi and T. Takahashi, *IEICE Trans. Electron.* **E87**, 227 (2004).
- <sup>6</sup>N. N. Greenwood and A. Earnshaw, *Chemistry of the Elements*, 2nd ed. (Butterworth-Heinemann, London, 1997).
- <sup>7</sup>D. Depla, S. Heirwegh, S. Mahieu, J. Haemers, and R. J. De Gryse, *J. Appl. Phys.* **101**, 013301 (2007).
- <sup>8</sup>S. Berg and T. Nyberg, *Thin Solid Films* **476**, 215 (2005).
- <sup>9</sup>S. Hashimoto, A. Tanaka, A. Murata, and T. Sakurada, *Surf. Sci.* **556**, 22 (2004).
- <sup>10</sup>J. F. Ziegler, J. P. Biersack, and M. D. Ziegler, *SRIM*, the stopping and range of ions in matter, Ziegler Scientific Company, 2006.
- <sup>11</sup>W. Eckstein and W. Moller, *Nucl. Instrum. Methods Phys. Res. B* **7-8**, 727 (1985).
- <sup>12</sup>R. Kelly, *Nucl. Instrum. Methods Phys. Res. B* **18**, 388 (1986).
- <sup>13</sup>E. Dullni, *Appl. Phys. A: Solids Surf.* **38**, 131 (1985).
- <sup>14</sup>G. V. Samsonov, *The Oxide Handbook*, 2nd ed. (IFI-Plenum, New York, 1982).
- <sup>15</sup>E. Dullni, *Nucl. Instrum. Methods Phys. Res. B* **2**, 610 (1984).